Electronic Supplementary Material (ESI) for Journal of Materials Chemistry A.
This journal is © The Royal Society of Chemistry 2023

Supporting Information

Activation in the Rate of Oxygen Release of $Sr_{0.8}Ca_{0.2}FeO_{3-\delta}$ Through Removal of Secondary Surface Species with Thermal Treatment in a CO_2-Free Atmosphere

Giancarlo Luongo, Alexander H. Bork, Paula M. Abdala, Yi-Hsuan Wu, Evgenia Kountoupi, Felix Donat and Christoph R. Müller**

Laboratory of Energy Science and Engineering, Department of Mechanical and Process Engineering, ETH Zurich, Leonhardstrasse 21, 8092 Zürich, Switzerland

*Corresponding authors: Dr. Felix Donat, email: donatf@ethz.ch; Prof. Christoph R. Müller, email: muelchri@ethz.ch

Keywords: chemical looping; air separation; oxygen carrier; perovskite; activation

1. Activation in the rate of oxygen release from $Sr_{1-x}Ca_xFeO_{3-\delta}$

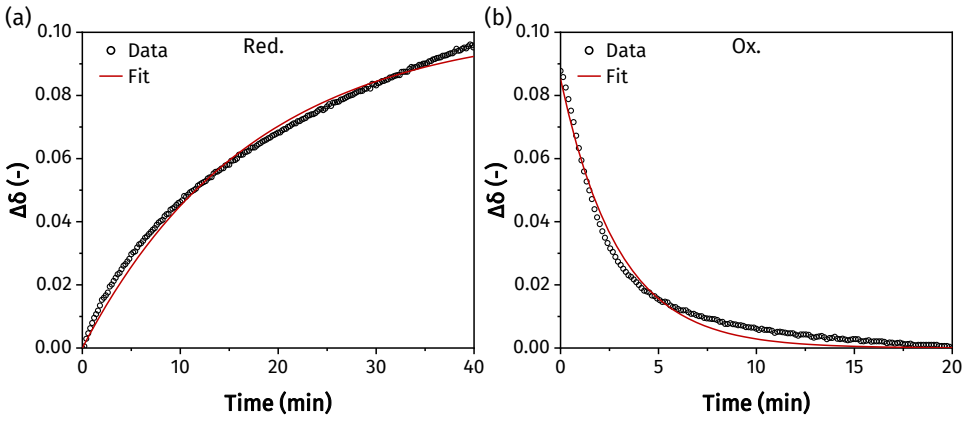

Figure S1 – Fitting of the change in oxygen non-stoichiometry Δδ during the (a) reduction and (b) oxidation steps of $Sr_{0.8}Ca_{0.2}FeO_{3-\delta}$ at 500 °C in first cycle.

Figure S2 shows the results of 10 redox cycles carried out with $SrFeO_{3-\delta}$, $Sr_{0.9}Ca_{0.1}FeO_{3-\delta}$ and $Sr_{0.75}Ca_{0.25}FeO_{3-\delta}$ to illustrate that an activation occurs for other compositions of the $Sr_{1-x}Ca_xFeO_{3-\delta}$ family. Note that here we focused only on phase pure perovskites, which are obtained when $0 \leq x \leq 0.25$, as reported in our previous work. [1] An increase in the rates of oxygen release was observed for all three samples at 500 °C, with the amount of oxygen released after 10 cycles of ~ 0.80 wt%, ~ 0.90 wt% and ~ 2.02 wt%, for $SrFeO_{3-\delta}$, $Sr_{0.9}Ca_{0.1}FeO_{3-\delta}$ and $Sr_{0.75}Ca_{0.25}FeO_{3-\delta}$, respectively. [1]

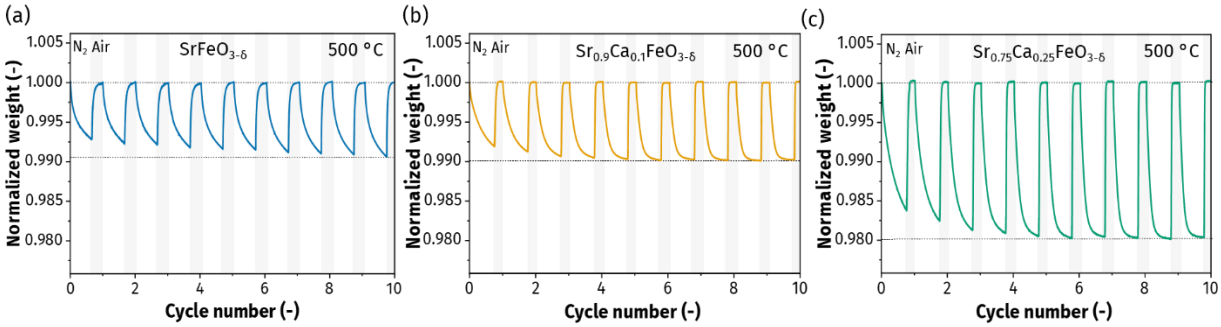

Figure S2 – Redox performance upon cycling. Normalized weight upon redox cycling (40 min reduction in N_2 and 20 min oxidation in air) collected in a TGA at 500 °C for (a) $SrFeO_{3-\delta}$, (b) $Sr_{0.9}Ca_{0.1}FeO_{3-\delta}$ and (c) $Sr_{0.75}Ca_{0.25}FeO_{3-\delta}$.

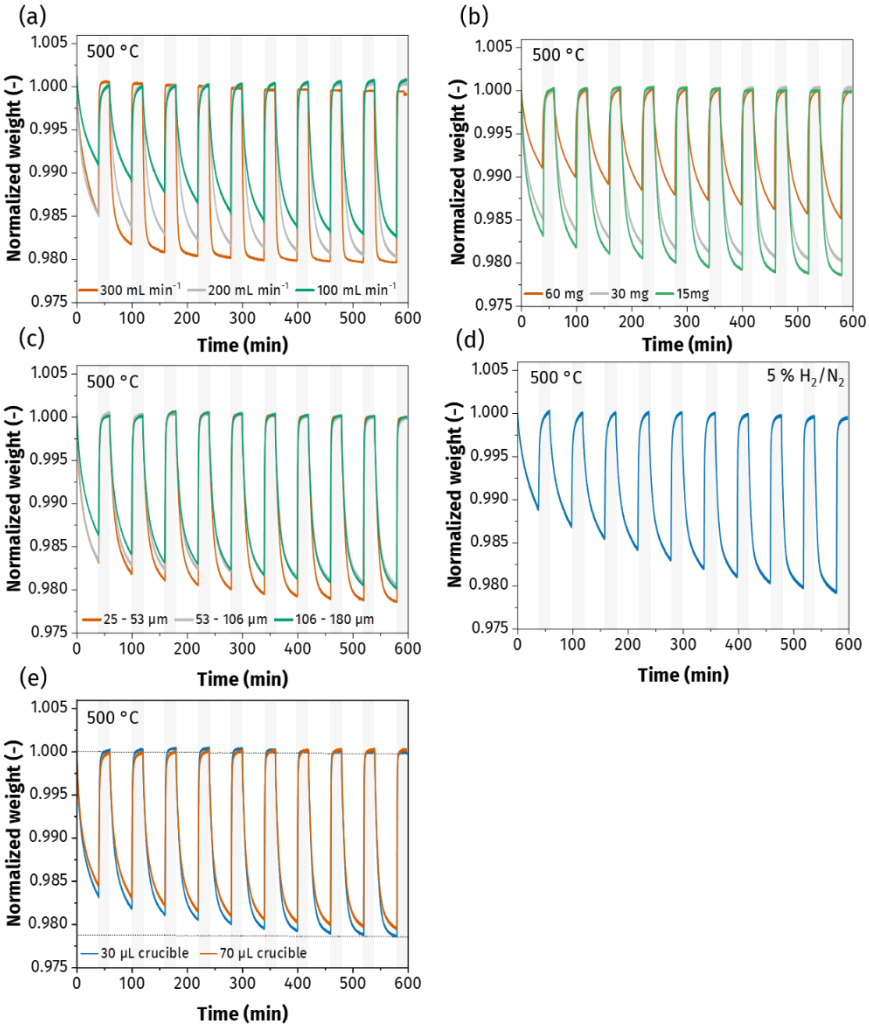

Figure S3 – Influence of different operating conditions on the increase in the rate of oxygen release. Normalized weight of $Sr_{0.8}Ca_{0.2}FeO_{3-\delta}$ upon redox cycling at 500 °C by using (a) different total flowrates (300 mL min^{-1}, 200 mL min^{-1}, 100 mL min^{-1}), (b) different total sample masses (60 mg, 30 mg, 15 mg), (c) different particle sizes (25 – 53 µm, 53 – 106 µm, 106 – 180 µm), (d) 5 % H_2/N_2 reducing atmosphere and (e) by using a shallow 30 µL or a 70 µL crucible.

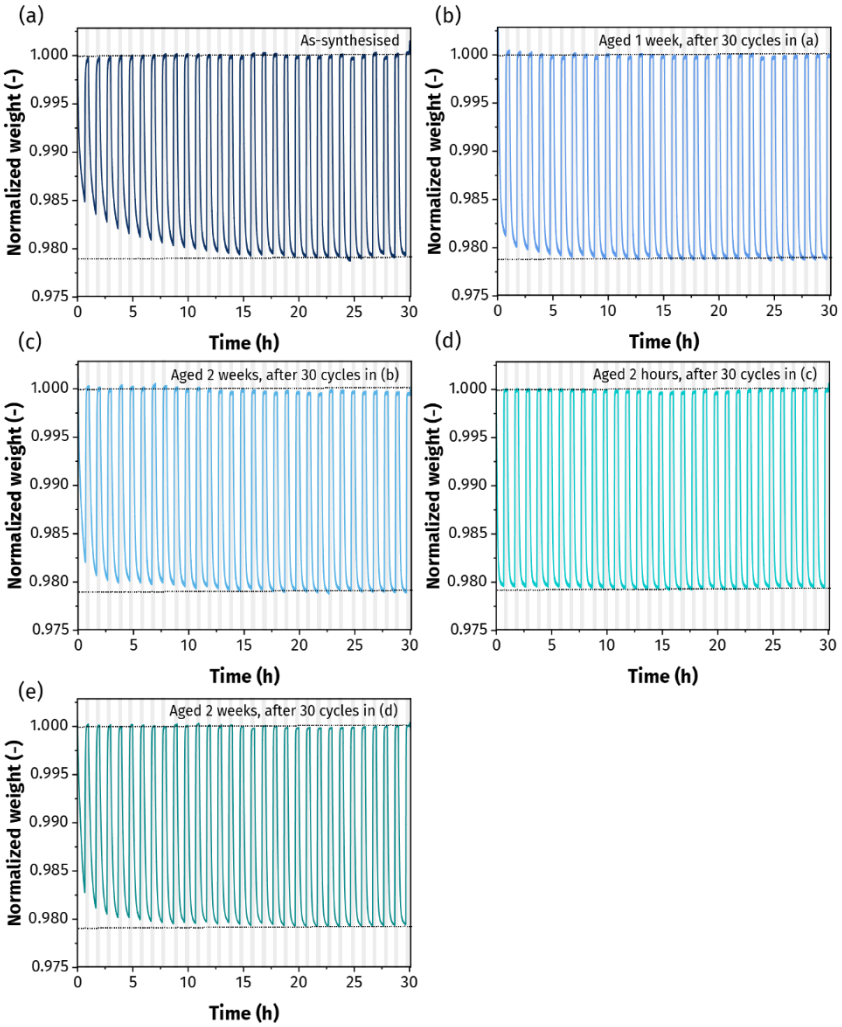

Figure S4 – The effect of aging at ambient conditions in a closed vial on the increase in the rate of oxygen release. Normalized weight upon redox cycling at 500 °C of the same sample when (a) as synthesized, (b) after aging for 1 week, (c) after aging for additional 2 weeks, (d) after aging for 2 hours after activation in (c), (e) after activation in (d) and aging for another 2 weeks.

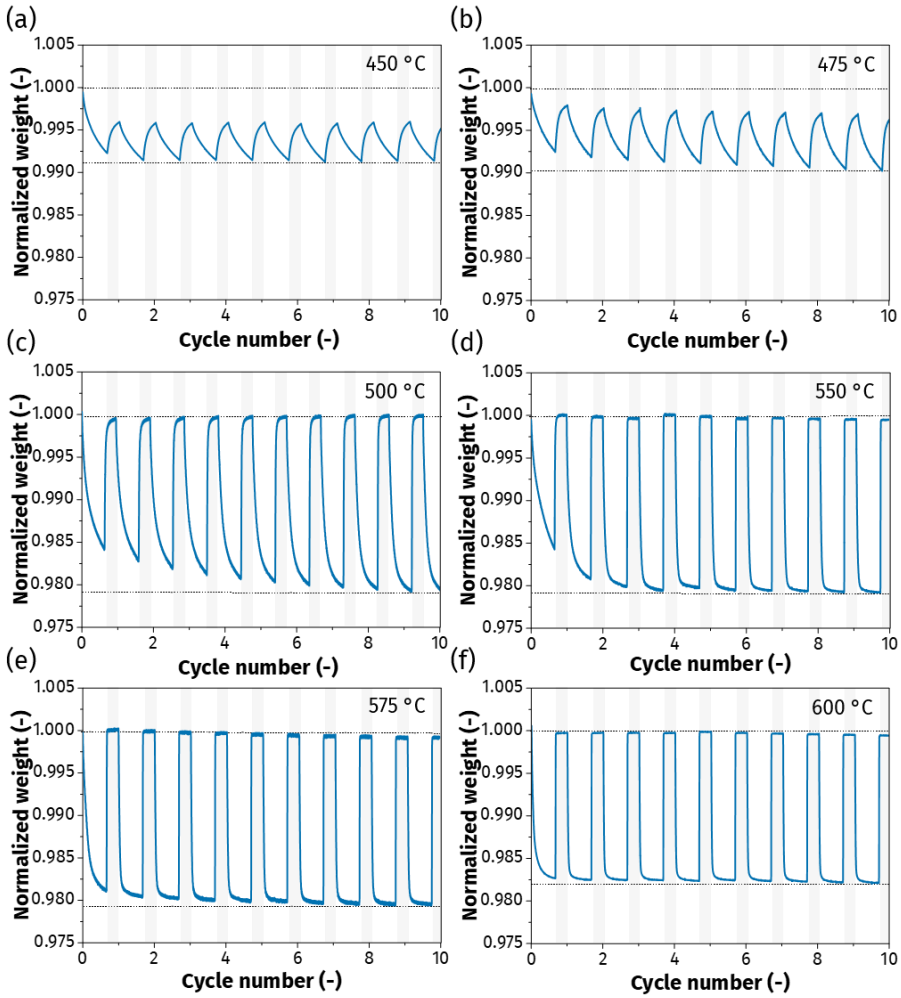

Figure S5 – The effect of the temperature on the increase in the rate of oxygen release. Normalized weight upon cycling at (a) 450 °C, (b) 475 °C, (c) 500 °C, (d) 550 °C, (e) 575 °C and (f) 600 °C.

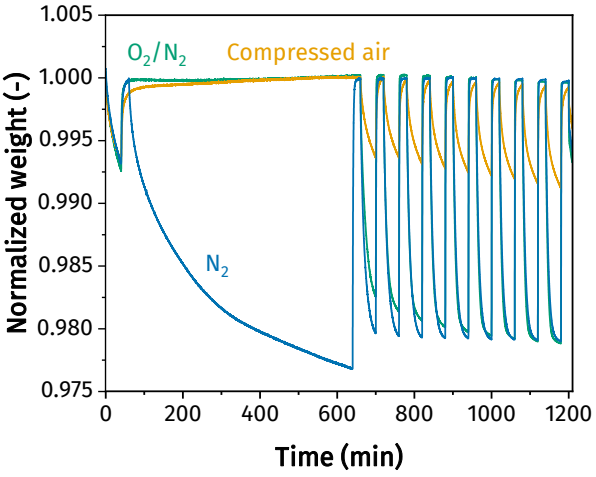

Figure S6 – Normalized weight of $Sr_{0.8}Ca_{0.2}FeO_{3-\delta}$ upon one redox cycle followed by exposure to N_2 for 10 h, synthetic air (O_2/N_2) or compressed air (containing small amounts of CO_2), and then nine redox cycles, with 40 min reduction in N_2 and 20 min oxidation in synthetic air or compressed air, at 500 °C.

Table S1 – Fitted parameters used for the calculation of the relaxation times of reaction and goodness of the fit for different TGA measurements.

Cycle number	Fitted parameters, 10 cycles, see Figure 1		
	τ_{RED}	a	R^2
1	5.7872	0.1904	0.98983
2	5.7872	0.1904	0.99607
3	5.7872	0.1904	0.99738
4	5.7872	0.1904	0.99809
5	5.7872	0.1904	0.99919
6	5.7872	0.1904	0.99896
7	5.7872	0.1904	0.99878
8	5.7872	0.1904	0.99906
9	5.7872	0.1904	0.99902
10	5.7872	0.1904	0.99904

Cycle number	Fitted parameters, As synthesized, see Figure S4a			Fitted parameters, 1 week, see Figure S4b		
	τ_{RED}	a	R^2	τ_{RED}	a	R^2
1	10.138	0.1507	0.98558	7.2424	0.21104	0.99772
2	8.661	0.15862	0.98303	5.6982	0.20187	0.99723
3	7.7509	0.16844	0.98422	5.411	0.20289	0.99715
4	7.254	0.1765	0.98572	5.2248	0.20462	0.99702
5	6.8704	0.18255	0.98637	5.1499	0.20305	0.99759
6	6.6678	0.18582	0.98976	5.0125	0.20347	0.99772
7	6.3449	0.19064	0.98988	4.9282	0.20317	0.99771
8	6.1233	0.19371	0.99122	4.7487	0.20625	0.99674
9	5.9406	0.19605	0.99231	4.6492	0.20588	0.99702
10	5.7114	0.19883	0.99294	4.5983	0.20452	0.99734
11	5.4414	0.20256	0.9918	4.4848	0.20586	0.99646
12	5.3044	0.20357	0.99271	4.455	0.20527	0.99684
13	5.1715	0.20333	0.99375	4.3698	0.20605	0.99616
14	5.0351	0.2053	0.99343	4.3543	0.20365	0.99692
15	4.8828	0.20748	0.99271	4.3024	0.20411	0.99649
16	4.7561	0.20846	0.99225	4.1934	0.20555	0.99515
17	4.7344	0.20793	0.9932	4.2607	0.20397	0.99587
18	4.5832	0.20943	0.99177	4.2811	0.20347	0.99561
19	4.4978	0.20907	0.99193	4.1839	0.20408	0.99485
20	4.4542	0.20794	0.99243	4.0762	0.2041	0.9937
21	4.3664	0.20741	0.9922	4.0123	0.20394	0.99331
22	4.2835	0.20795	0.99112	4.0087	0.20156	0.99413
23	4.2172	0.20736	0.99083	3.93	0.20275	0.99294
24	4.151	0.20745	0.98994	3.8531	0.20334	0.99131
25	3.9839	0.21194	0.98433	3.8069	0.20238	0.99117
26	4.0781	0.20621	0.98972	3.7591	0.20115	0.99123
27	3.9904	0.20749	0.98768	3.7393	0.19999	0.9908
28	3.9877	0.20654	0.98752	3.7133	0.19938	0.9909
29	3.9365	0.2065	0.98665	3.6267	0.20147	0.98798
30	3.887	0.20654	0.98558	3.5773	0.20122	0.98705

Cycle number	Fitted parameters, 2 weeks, see Figure S4c			Fitted parameters, 2 hours, see Figure S4d		
	T_{RED}	a	R^2	T_{RED}	a	R^2
1	14.575	0.2077	0.99055	5.7342	0.22202	0.99759
2	10.363	0.20864	0.99834	4.8843	0.21925	0.99848
3	8.6285	0.21093	0.99836	4.8235	0.21831	0.99842
4	7.8306	0.21102	0.9987	4.7527	0.21749	0.99836
5	7.293	0.21182	0.99882	4.6719	0.21898	0.99845
6	6.8525	0.21331	0.9986	4.6642	0.21753	0.9985
7	6.5602	0.2135	0.99868	4.6363	0.21743	0.99852
8	6.2089	0.21671	0.9979	4.5362	0.21936	0.99854
9	6.159	0.21396	0.99852	4.4964	0.2195	0.99841
10	5.9359	0.21441	0.99831	4.4509	0.21983	0.99829
11	5.7531	0.21638	0.99789	4.4281	0.22025	0.99812
12	5.6083	0.2153	0.99807	4.3957	0.21894	0.99801
13	5.4978	0.21564	0.99787	4.383	0.21857	0.99802
14	5.3346	0.21667	0.99726	4.3174	0.21944	0.9975
15	5.1824	0.21702	0.99703	4.3059	0.2179	0.99757
16	5.099	0.21666	0.99691	4.2783	0.21811	0.99731
17	4.9806	0.21728	0.99641	4.2227	0.21997	0.99644
18	4.9743	0.21519	0.99703	4.2049	0.21962	0.996
19	4.8672	0.2153	0.99654	4.184	0.21926	0.99562
20	4.797	0.21653	0.99569	4.1464	0.21952	0.99496
21	4.7467	0.21579	0.9956	4.1764	0.21672	0.99582
22	4.6958	0.2153	0.99537	4.0851	0.21889	0.99419
23	4.5837	0.21743	0.99375	4.0799	0.21709	0.99453
24	4.5809	0.21533	0.99423	4.0503	0.21687	0.99386
25	4.4867	0.21741	0.99228	3.9986	0.21727	0.99312
26	4.4732	0.21647	0.99235	3.9451	0.2183	0.99168
27	4.4067	0.21738	0.99105	3.8825	0.21883	0.98995
28	4.3398	0.21779	0.98988	3.8612	0.21802	0.99011
29	4.3222	0.21606	0.99027	3.8605	0.2165	0.99015
30	4.2483	0.21687	0.98869	3.8115	0.21743	0.9884

Cycle number	Fitted parameters, 2 weeks, see Figure S4e		
	T_{RED}	a	R^2
1	24.038	0.23307	0.99392
2	12.795	0.2072	0.99787
3	10.364	0.20822	0.99847
4	9.035	0.21028	0.99844
5	8.2775	0.20691	0.99817
6	7.6922	0.21133	0.99859
7	7.2962	0.21119	0.99868
8	6.969	0.21136	0.99859
9	6.6969	0.21154	0.99851
10	6.4747	0.21109	0.99852
11	6.2754	0.21174	0.99822
12	6.0947	0.21193	0.99806
13	5.9445	0.21181	0.99795
14	5.8213	0.2121	0.99772
15	5.703	0.21179	0.99753
16	5.6257	0.21145	0.99745

17	5.6749	0.20698	0.99792
18	5.4312	0.21079	0.9969
19	5.3566	0.21067	0.99664
20	5.2759	0.21016	0.99633
21	5.2232	0.20996	0.99606
22	5.155	0.2098	0.99576
23	5.103	0.20922	0.99541
24	5.0647	0.20919	0.9951
25	5.0003	0.20897	0.9946
26	4.9459	0.20831	0.99435
27	4.9022	0.208	0.99396
28	4.8453	0.20813	0.99318
29	4.7941	0.2077	0.99289
30	4.741	0.20753	0.9922

Cycle number	**Fitted parameters, CO_2_1%, see Figure 2a**			**Fitted parameters, CO_2_5%, see Figure 2a**		
	T_{RED}	**a**	**R^2**	**T_{RED}**	**a**	**R^2**
1	15.934	0.077424	0.99658	12.024	0.13328	0.98967
2	11.222	0.079306	0.98905	9.1614	0.14535	0.99022
3	11.004	0.080069	0.99148	8.0088	0.15305	0.98448
4	9.9637	0.080689	0.98897	7.7031	0.15939	0.98726
5	10.158	0.082546	0.99214	7.3681	0.16535	0.98759
6	18.344	0.085848	0.99937	19.646	0.18186	0.99904
7	10.086	0.081742	0.98928	7.4402	0.16644	0.9908
8	9.6944	0.082786	0.98915	6.7818	0.17057	0.99129
9	9.111	0.083428	0.98755	6.5176	0.17333	0.99019
10	8.8739	0.084327	0.98801	6.3721	0.17641	0.98995

Cycle number	**Fitted parameters, CO_2_10%, see Figure 2a**			**Fitted parameters, CO_2_50%, see Figure 2a**		
	T_{RED}	**a**	**R^2**	**T_{RED}**	**a**	**R^2**
1	9.7886	0.14222	0.98759	9.7727	0.14441	0.98833
2	8.4754	0.14961	0.9856	8.5107	0.15236	0.98695
3	7.823	0.15841	0.9862	7.8432	0.15979	0.98685
4	7.4474	0.16431	0.98759	8.1446	0.16593	0.99589
5	7.3007	0.16772	0.99005	7.2471	0.17012	0.99226
6	22.854	0.19763	0.99847	5096.5	22.232	0.99324
7	7.242	0.17006	0.98974	7.3896	0.16916	0.9922
8	6.6039	0.17434	0.99078	6.4553	0.17372	0.98981
9	6.4447	0.17496	0.99174	6.2611	0.17699	0.99022
10	6.2994	0.17808	0.99148	6.1565	0.17731	0.99057

Cycle number	**Fitted parameters, 450 °C, see Figure S5a**					
	T_{RED}	**T_{OX}**	**a**	**b**	**$R^2_{,RED}$**	**$R^2_{,OX}$**
1	22.036	5.8369	0.043112	0.021878	0.99696	0.99555
2	23.864	6.1412	0.035327	0.023252	0.99586	0.996
3	23.602	6.2755	0.034173	0.023275	0.99561	0.99671
4	23.642	6.2036	0.034161	0.023737	0.99435	0.99491
5	24.217	6.356	0.034292	0.02386	0.99612	0.99617
6	23.622	6.3161	0.034418	0.023941	0.9946	0.99543

7	23.887	6.2821	0.034372	0.024182	0.99552	0.99522
8	23.949	6.2503	0.034262	0.024341	0.99506	0.99496
9	23.616	6.4856	0.034035	0.024665	0.99472	0.99624
10	22.697	-	0.0333	-	0.99431	-

Cycle number	**Fitted parameters, 475 °C, see Figure S5b**					
	τ_{RED}	**τ_{OX}**	**a**	**b**	**$R^2_{,RED}$**	**$R^2_{,OX}$**
1	20.248	4.6995	0.068775	0.050057	0.9973	0.99684
2	17.823	4.6442	0.057883	0.052121	0.99612	0.99754
3	16.857	4.6157	0.057251	0.053061	0.99457	0.997
4	16.141	4.5951	0.057166	0.053679	0.99359	0.99695
5	15.982	4.5974	0.05763	0.054336	0.99335	0.9967
6	16.183	4.5014	0.058433	0.054727	0.9944	0.99628
7	15.603	4.4788	0.058551	0.055007	0.99337	0.99542
8	15.541	4.4114	0.059655	0.055518	0.99289	0.99522
9	15.159	4.3958	0.060542	0.056036	0.99215	0.9951
10	14.868	-	0.060611	-	0.99209	-

Cycle number	**Fitted parameters, 500 °C, see Figure S5c**					
	τ_{RED}	**τ_{OX}**	**a**	**b**	**$R^2_{,RED}$**	**$R^2_{,OX}$**
1	15.28	2.9481	0.095772	0.085185	0.99482	0.98162
2	11.858	2.7401	0.09664	0.095022	0.9879	0.97738
3	10.911	2.4802	0.10475	0.10348	0.9877	0.97376
4	10.356	2.2335	0.11273	0.11092	0.98851	0.97224
5	9.7018	2.0676	0.12048	0.11717	0.98792	0.96819
6	9.2381	1.9252	0.12812	0.12281	0.9878	0.96557
7	8.8418	1.7653	0.13484	0.12841	0.98838	0.96918
8	8.4963	1.6496	0.14132	0.13394	0.98896	0.96868
9	8.1397	1.517	0.14801	0.13898	0.98849	0.97241
10	7.9161	-	0.15378	-	0.98957	-

Cycle number	**Fitted parameters, 550 °C, see Figure S5d**					
	τ_{RED}	**τ_{OX}**	**a**	**b**	**$R^2_{,RED}$**	**$R^2_{,OX}$**
1	14.336	0.47098	0.19538	0.1952	0.98975	0.99536
2	3.5546	0.32146	0.17827	0.19851	0.99638	0.99279
3	2.7054	0.27787	0.18167	0.1885	0.99791	0.99129
4	2.3724	0.26078	0.18136	0.1756	0.99805	0.98989
5	2.1702	0.24984	0.18275	0.1628	0.99788	0.98957
6	2.0367	0.24244	0.18098	0.14992	0.99772	0.98923
7	1.9205	0.23636	0.18151	0.13749	0.99741	0.98911
8	1.8373	0.23166	0.17963	0.12602	0.99709	0.9894
9	1.7618	0.2273	0.17891	0.11496	0.99665	0.98896
10	1.7004	-	0.17864	-	0.99583	-

Cycle number	**Fitted parameters, 575 °C, see Figure S5e**					
	τ_{RED}	**τ_{OX}**	**a**	**b**	**$R^2_{,RED}$**	**$R^2_{,OX}$**
1	5.6079	0.38419	0.18244	0.23916	0.99626	0.95223
2	1.7643	0.33604	0.18627	0.23379	0.99527	0.9492
3	1.49	0.32226	0.18665	0.22326	0.9963	0.94764

4	1.3484	0.3173	0.1894	0.21206	0.99636	0.94788
5	1.268	0.3183	0.18682	0.2016	0.99596	0.94721
6	1.1999	0.30877	0.18663	0.18937	0.99536	0.9485
7	1.15	0.30273	0.18646	0.17775	0.99406	0.94813
8	1.1036	0.29842	0.18569	0.16665	0.99282	0.94861
9	1.0625	0.29573	0.18563	0.15688	0.99083	0.95027
10	1.0315	-	0.18515	-	0.98783	-

Cycle number	**Fitted parameters, 600 °C, see Figure S5f**					
	τ_{RED}	**τ_{OX}**	**a**	**b**	**$R^2_{,RED}$**	**$R^2_{,OX}$**
1	2.2641	0.30381	0.17752	0.23322	0.963	0.94643
2	1.1136	0.28914	0.17869	0.22365	0.99195	0.94547
3	0.98292	0.28393	0.17906	0.21102	0.99321	0.9457
4	0.90854	0.27805	0.17881	0.19769	0.99304	0.94666
5	0.85258	0.27424	0.17857	0.18493	0.99264	0.94725
6	0.81223	0.26994	0.17839	0.17318	0.991	0.94783
7	0.7775	0.26736	0.17793	0.16182	0.98876	0.94839
8	0.74679	0.264	0.17806	0.15072	0.9851	0.94979
9	0.7231	0.26131	0.17699	0.14066	0.98085	0.95019
10	0.70081	-	0.17716	-	0.97312	-

2. Bulk perovskite structure and changes upon redox cycling

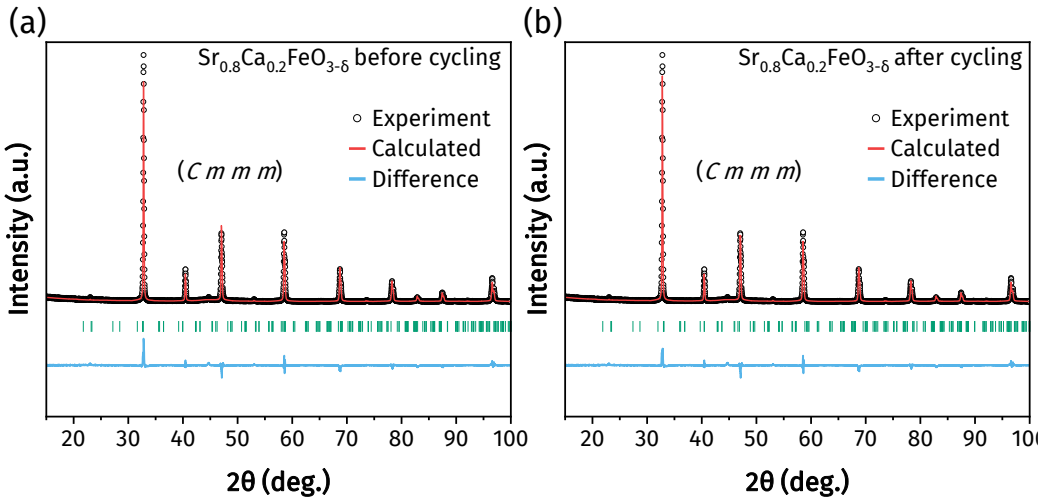

Figure S7 – Full pattern refinement (Rietveld analysis) of $Sr_{0.8}Ca_{0.2}FeO_{3-\delta}$ before and after redox cycling (30 redox cycles in a TGA at 500 °C). The calculated lattice parameters were a = 10.906(4) Å, b = 7.674(6) Å and c = 5.472(4) Å for the sample before cycling and a = 10.901(6) Å, b = 7.671(2) Å and c = 5.469(5) Å for the sample after cycling.

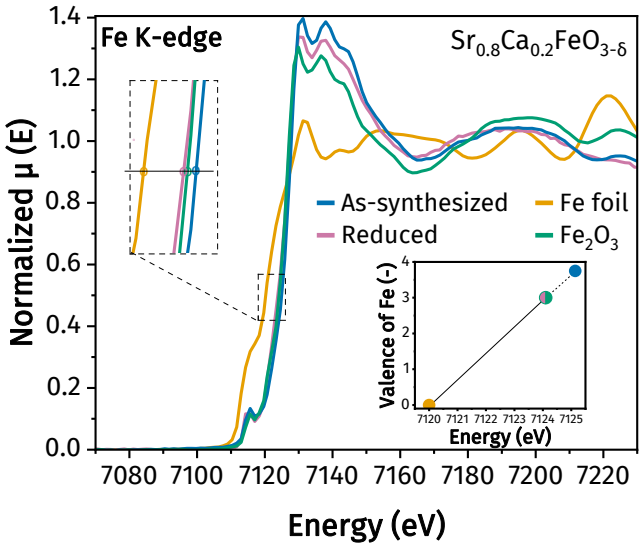

Figure S8 – Fe K-edge XANES of $Sr_{0.8}Ca_{0.2}FeO_{3-\delta}$ as synthesized and reduced (after 40 min in N_2 at 500 °C), together with Fe foil and Fe_2O_3 that acted as references. The inset plot on the top left side shows a zoom into the edge position. The inset on the bottom right plots the oxidation state of the materials against the edge positions (determined at half of the normalized intensity [2]), considering Fe foil (Fe^0) and Fe_2O_3 (Fe^{+3}) as the respective references. The average valance state of Fe in $Sr_{0.8}Ca_{0.2}FeO_{3-\delta}$ as synthesized was extrapolated by using a linear relationship and was found to be between +4 and +3 (ca. $Fe^{+3.76}$), giving an indirect measurement of the initial non-stoichiometry of approximately δ = 0.14.

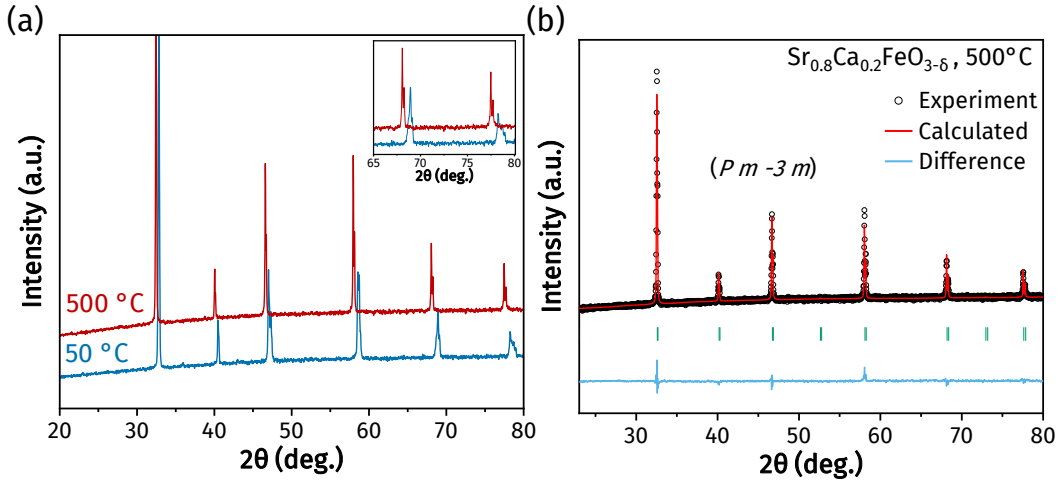

Figure S9 – Structural change of the perovskite from orthorhombic to cubic upon heating to 500 °C in air. (a) In-situ XRD patterns of $Sr_{0.8}Ca_{0.2}FeO_{3-\delta}$ collected at 50 °C and 500 °C. (b) Full pattern refinement (Rietveld analysis) of $Sr_{0.8}Ca_{0.2}FeO_{3-\delta}$ at 500 °C. The calculated lattice parameters were a = b = c = 3.898(8) Å. At 50 °C the structure was indexed with an orthorhombic space group, and at 500°C the cubic *Pm*-3*m* space group explained all reflections. The inset in (a) magnifies the difference in the high-order reflections for the patterns collected at 50 °C and 500 °C.

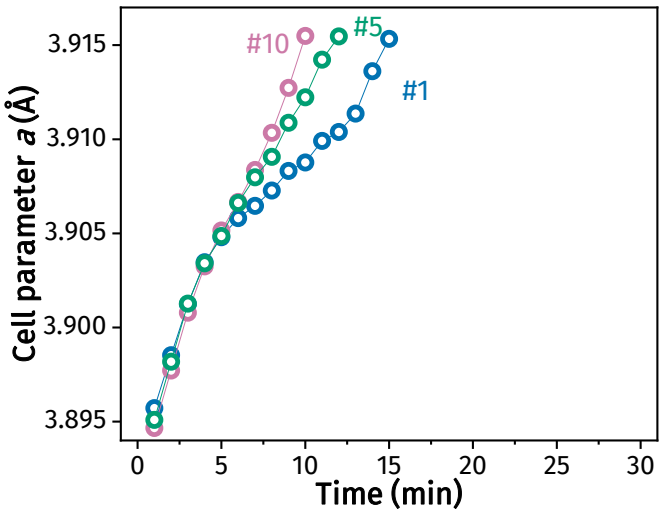

Figure S10 – Evolution of the cell parameter of the perovskite $Sr_{0.8}Ca_{0.2}FeO_{3-\delta}$ with time under N_2 at 500 °C.

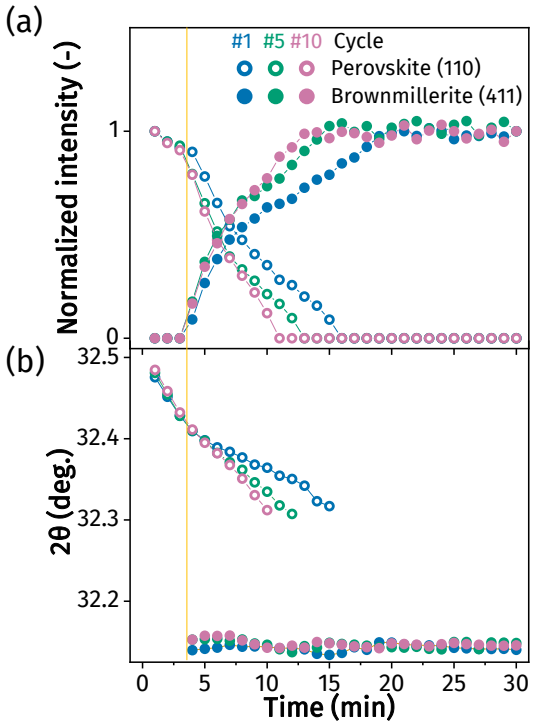

Figure S11 – Evolution of (a) the integrated intensity normalized with respect to the maximum observed intensity and (b) peak position of the perovskite (110) and brownmillerite (411) peaks, related to the measurements shown in Figure 4. The yellow vertical line indicates the onset of the phase transition from perovskite to brownmillerite at ~ 4 min.

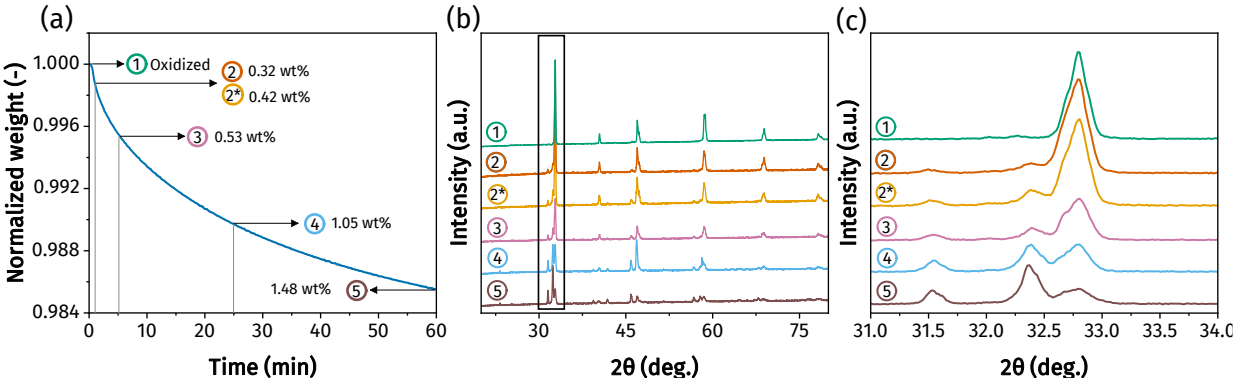

Figure S12 – Ex-situ studies of the structural evolution of $Sr_{0.8}Ca_{0.2}FeO_{3-\delta}$ at different degrees of reduction. (a) Normalized weight upon reduction in N_2 at 500 °C in the TGA. Samples were collected at different times of reduction (1 @0 min, 2 and 2* @1 min, 3 @5 min, 4 @25 min, 5 @60 min) with the corresponding (1 – 5) XRD patterns (collected at room temperature and ambient air) shown in (b), and magnified in (c) in the 2θ range 31 – 34 °. The XRD pattern corresponding to point 2* is that of an activated sample (i.e. treatment in synthetic air at 600 °C for 2 h), collected after the same time as point 2. Note that the evolution of the perovskite peak observed in (c) (i.e. at room temperature) is different from the one observed with in-situ XRD measurements at 500 °C (Figure 4). Here, we observe a splitting of the perovskite peak upon reduction, while at 500 °C the perovskite peak only shifts gradually to lower angles, without any splitting. This is because at room temperature the perovskite has an orthorhombic structure, while under operating conditions (500 °C), i.e. the temperature at which in-situ XRD patterns were collected, the perovskite has a cubic structure.

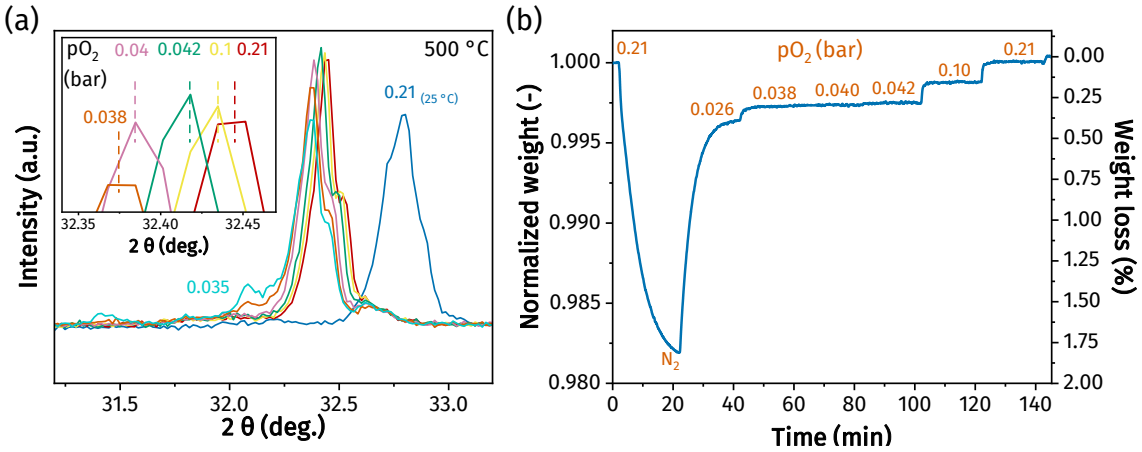

Figure S13 – Change in the peak position of the perovskite peak (110) before the onset of the phase transition from perovskite to brownmillerite and the corresponding amount of oxygen release. (a) In-situ XRD patterns of $Sr_{0.8}Ca_{0.2}FeO_{3-\delta}$ at 500 °C at different pO_2 obtained by using mixtures of air and N_2 (total flow rate 200 mL min^{-1}). The scans were collected 10 min after the change in the gas environment. (b) TGA measurement at 500 °C at different pO_2 obtained by using mixtures of compressed air and N_2 (total flow rate 150 mL min^{-1}). Each pO_2 step was 20 min.

3. Surface analysis

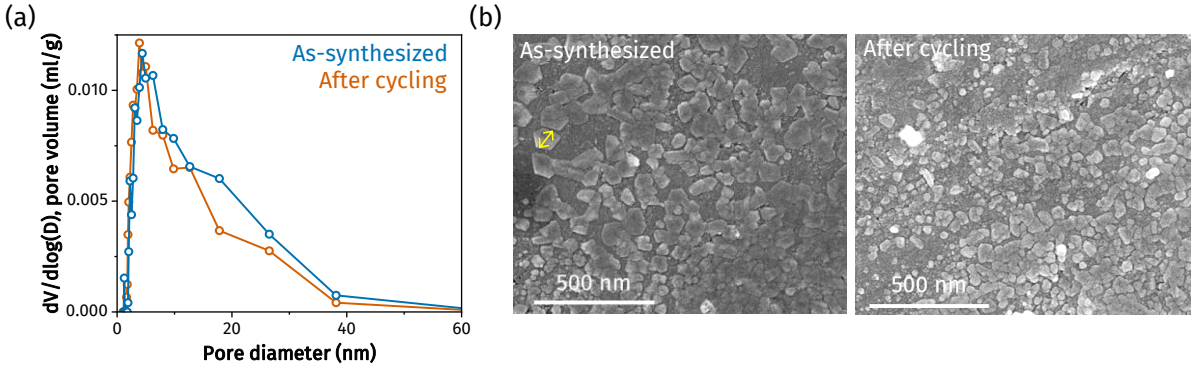

Figure S14 – Textural properties of $Sr_{0.8}Ca_{0.2}FeO_{3-\delta}$. (a) Pore volume distribution and (b) HR-SEM of the as-synthesized sample and after 10 redox cycles at 500 °C.

Table S2 – Position and intensity of the peaks in the Sr 3d, O 1s, Fe 2p and C 1s XPS spectra.

Sample	Name	Position (eV)	Intensity
Air-tight	Sr3d	133.1	10819
	O1s	531.2	13784
	Fe2p	710.4	9305
	C1s	289	165
CO_2-treated	Sr3d	133.1	10824
	O1s	531.3	13805
	Fe2p	710.4	9309
	C1s	289.05	4651
As-synthesized	Sr3d	133.1	10818
	O1s	531.3	13808
	Fe2p	710.4	9310

	C1s	289.05	4622
First cycle	Sr3d	133.1	10821
	O1s	531.3	13804
	Fe2p	710.4	9308
	C1s	289.05	4602
Third cycle	Sr3d	133.1	10821
	O1s	531.3	13799
	Fe2p	710.4	9308
	C1s	289.05	4594
Fifth cycle	Sr3d	133.1	10821
	O1s	531.3	13787
	Fe2p	710.4	9306
	C1s	289.05	4588
Tenth cycle	Sr3d	133.1	10819
	O1s	531.3	13786
	Fe2p	710.4	9306
	C1s	289.05	4497

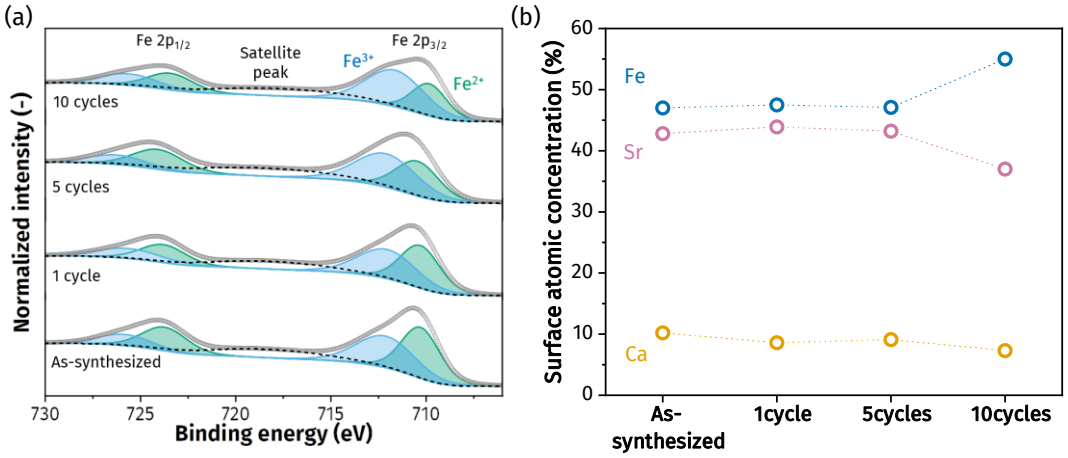

Figure S15 – (a) Fe XPS spectra of the as-synthesized $Sr_{0.8}Ca_{0.2}FeO_{3-\delta}$ and after 1, 5 and 10 redox cycles in the TGA. (b) Atomic concentration at the surface of the sample as synthesized and after 1, 5 and 10 redox cycles measured with XPS.

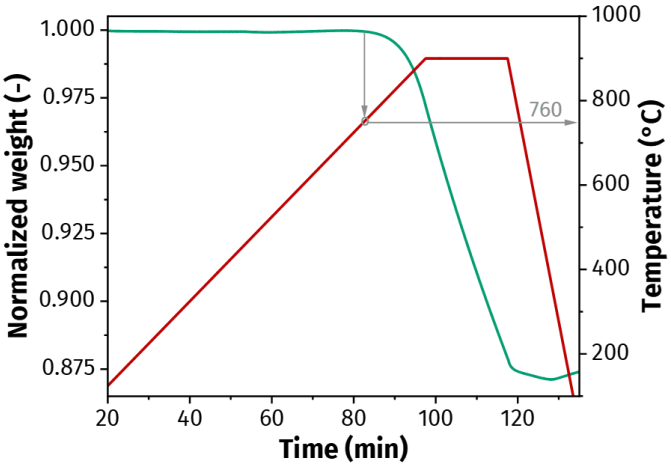

Figure S16 – Decomposition of $SrCO_3$.Temperature programmed reduction of $SrCO_3$ heating to 900 °C at 5 °C min^{-1} in N_2 (150 mL min^{-1}) and held at 900 °C for 30 min. The onset temperature of the decomposition of $SrCO_3$ is at 760 °C.

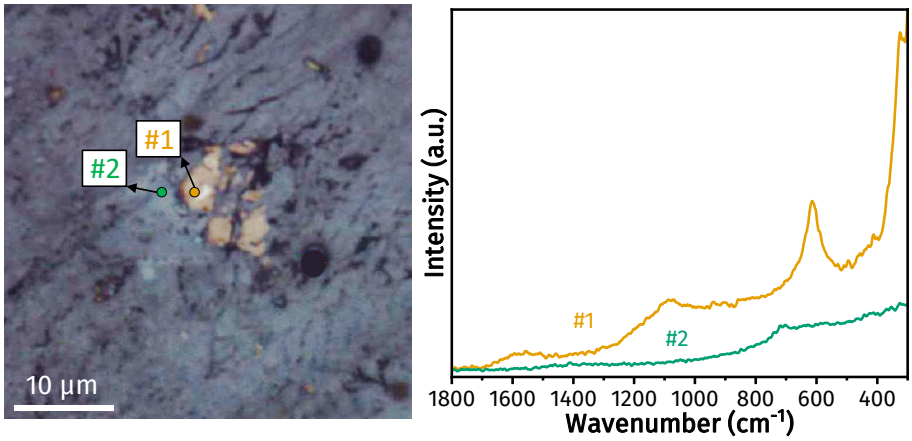

Figure S17 – Optical microscope image collected by using 100× optical magnification at 25 °C and corresponding Raman spectra, collected by using 50× optical magnification, of the as-synthesized $Sr_{0.8}Ca_{0.2}FeO_{3-\delta}$, ground to fine particles and pelletized.

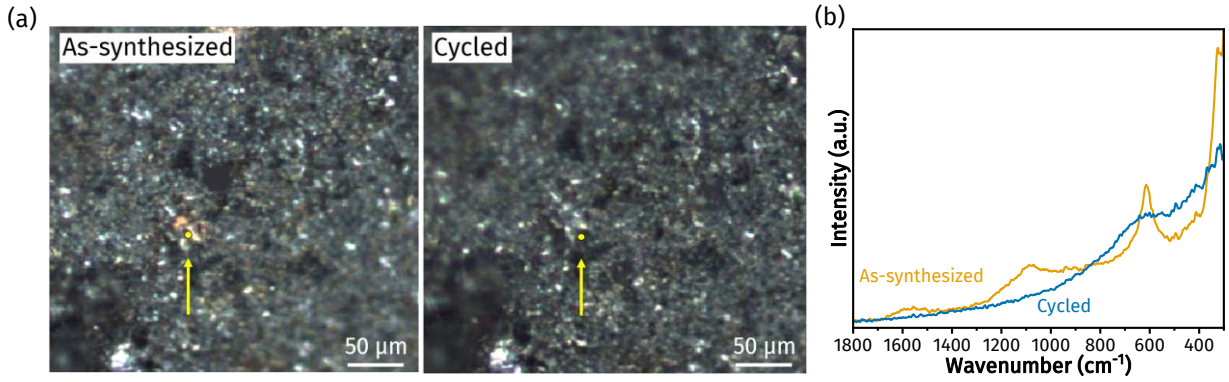

Figure S18 – (a) Optical microscope image of the as-synthesized and cycled sample collected at 25 °C by using 10× optical magnification; (b) corresponding Raman spectra. The as-synthesized sample was ground to fine particles and pelletized. The sample was heated in the in-situ Raman cell to 700 °C in air (heating rate 10 °C min^{-1}), then redox cycled once in N_2 (40 min) and air (20 min), and cooled down to 25 °C.

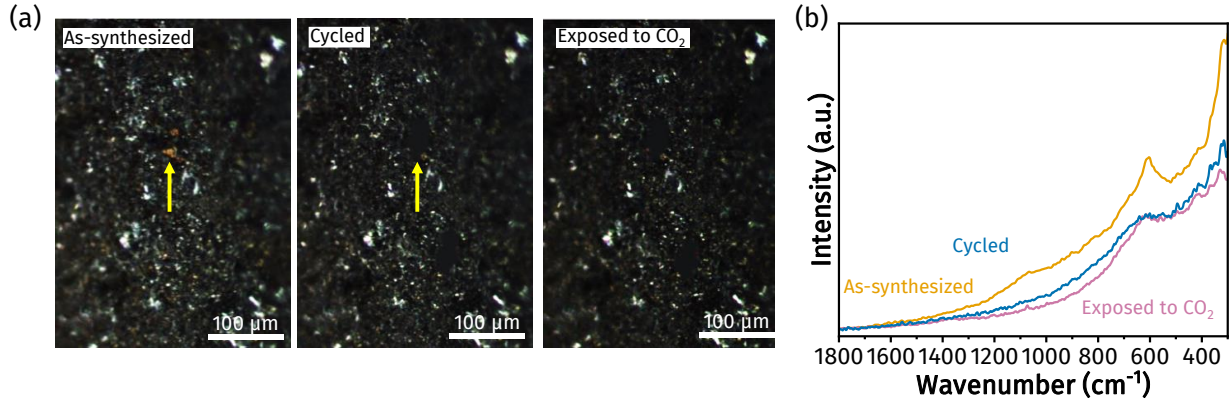

Figure S19 – (a) Optical microscope images collected by using 10× optical magnification of: As-synthesized sample at 25 °C; the sample heated to 700 °C in air (heating rate 10 °C min^{-1}), and then redox cycled once in N_2 (40 min) and air (20 min); the sample after exposure at 500 °C to CO_2 for 20 min; (b) corresponding Raman spectra.

References

[1] Luongo, G., Donat, F., Müller, C. R., *Physical Chemistry Chemical Physics*, **2020**, *22*(17), pp.9272-9282.

[2] Tamai, K., Hosokawa, S., Kato, K., Asakura, H., Teramura, K., Tanaka, T., *Physical Chemistry Chemical Physics*, **2020**, 22(42), pp.24181-24190.